

Dynamics of matter solitons in weakly modulated optical lattices

V.A. Brazhnyi^{1,*} V.V. Konotop^{1,2,†} and V. Kuzmiak^{3‡}

¹ Centro de Física Teórica e Computacional, Universidade de Lisboa,
Complexo Interdisciplinar, Av. Prof. Gama Pinto 2, Lisbon 1649-003, Portugal

² Departamento de Física, Universidade de Lisboa,
Campo Grande, Ed. C8, Piso 6, Lisboa 1749-016, Portugal

³ Institute of Radio Engineering and Electronics, Czech Academy of Sciences, Chaberska 57, 182 51 Prague 8, Czech Republic

We demonstrate a possibility of management of matter solitons in Bose-Einstein condensates by means of smooth modulations of optical lattices. In particular, we discuss effects of acceleration and oscillations in linearly and parabolically modulated lattices, as well as interaction of matter solitons with localized lattice defects.

PACS numbers:

Realization of Bose-Einstein condensate (BEC) in an optical lattice [1] originated intensive experimental and theoretical studies [2, 3, 4, 5] of the phenomenon. One of the main features of the presence of periodicity is the appearance of a band structure in the spectrum of the underlying linear system, i.e. of a BEC without interatomic interactions. Such spectrum is responsible for a number of effects, including formation of gap solitons [6], Landau-Zener tunneling [7], Bloch oscillations [1, 8], and soliton acceleration [8] and stabilization [9]. These effects can be considered as quasi-linear, in the sense they are based on the properties of the linear system, and in particular on a concept of the effective mass that takes into account the wave character of the phenomenon and that is why also can be referred to as the group velocity dispersion. In practice, laser lattices are never perfect. In particular, they are imposed simultaneously with additional potentials, a magnetic trap being a typical example which was numerically investigated in [10].

In this paper we present analysis of the BEC dynamics in a periodic potential perturbed in another way: namely, smoothly modulated. Then the band gap structure is still preserved but is deformed by the modulation. In particular, we show that this is a way of managing the dynamics of matter waves - making them accelerating, oscillating, etc.

To explain the physics of the phenomenon let us consider a trap potential which can be written down in the form $\frac{m}{2}(\omega_{\parallel}^2 x^2 + \omega_0^2 y^2 + \omega_0^2 z^2) + V_{\epsilon}(x)$. The first part describes a magnetic trap with ω_{\parallel} and ω_0 being the longitudinal and transverse linear oscillator frequencies. The condensate is chosen to have a cigar shape with the aspect ratio satisfying the relation $\omega_{\parallel}/\omega_0 \ll a_0^2/\xi^2 \ll 1$ (a_0 and ξ being the transverse linear oscillator length and the healing length, respectively). We are interested in excitations of a BEC having characteristic scales of order of the healing length and having a relatively small

amplitude, what allows us to neglect the term $\frac{m}{2}\omega_{\parallel}^2 x^2$. The potential $V_{\epsilon}(x)$, where ϵ is a deformation parameter controlling the potential shape, describes smoothly modulated optical trap and will be assumed to have the form $V_{\epsilon}(x) \equiv f(\epsilon^{3/2}x)V_0(x)$, where $V_0(x) = V_0(x + L)$ is an unperturbed lattice having a period L of order of the linear oscillator length a_0 and $f(\epsilon^{3/2}x)$ is a smooth modulation such that $f(0) = 1$. A smoothness in the present context means slow variation on the scale of the healing length, or in other words $\epsilon \sim a_0/\xi$. Then, one can apply the multiple-scale expansion in order to reduce the dynamics of the BEC to an effectively one-dimensional (1D) nonlinear Schrödinger (NLS) equation with slowly varying effective mass [6], $m_{\alpha} \equiv m_{\alpha}(\epsilon^{1/2}X) = [\partial^2 \mathcal{E}_{\alpha}(k; \epsilon^{1/2}X)/\partial k^2]^{-1}$, and the group velocity of the carrier wave $v_{\alpha} = \partial \mathcal{E}_{\alpha}(k; \epsilon^{1/2}X)/\partial k$:

$$i\psi_T + iv_{\alpha}\psi_X = -(2m_{\alpha})^{-1}\psi_{XX} + \sigma|\psi|^2\psi. \quad (1)$$

Hereafter α and k stand for a number of the zone and for the dimensionless wave vector in the first Brillouin zone (BZ), $\sigma = \text{sign } a_s$, a_s being the s-wave scattering length and we have passed to dimensionless slow variables: $X = \epsilon x/a_0 = \epsilon \tilde{x}$ and $T = \epsilon^2 \omega_0 t = \epsilon^2 \tilde{t}$. Taking into account smoothness of the potential, the spectrum, $\mathcal{E}_{\alpha}(k; \epsilon^{3/2}\tilde{x})$ in some point of the space, say $x = x_0$, can be computed from the linear eigenvalue problem ($\tilde{x}_0 = x_0/a_0$)

$$\frac{d^2\varphi_{nk}}{d\tilde{x}^2} + \left[\mathcal{E}_{\alpha}(k; \epsilon^{3/2}\tilde{x}_0) - f(\epsilon^{3/2}\tilde{x}_0)V_0(\tilde{x}) \right] \varphi_{nk} = 0. \quad (2)$$

In order to get qualitative picture of effects observable in the matter wave dynamics, in numerical simulations we explore a quasi-1D model for the low-density BEC with a negative scattering length $\sigma = -1$ which has the form of the NLS equation

$$i\psi_{\tilde{t}} = -\psi_{\tilde{x}\tilde{x}} + f(\epsilon^{3/2}\tilde{x})V_0(\tilde{x})\psi - |\psi|^2\psi. \quad (3)$$

In the case of homogeneous lattice, i. e. in (3) with $f(x) \equiv 1$, there exists a solitary wave solution (bright matter soliton) which can be found by means of the stationary ansatz $\psi(\tilde{x}, \tilde{t}) = u(\tilde{x})e^{-i\mathcal{E}\tilde{t}}$, where $u(\tilde{x})$ is a real valued function satisfying the equation as follows

$$u_{\tilde{x}\tilde{x}} + [\mathcal{E} - V_0(\tilde{x})]u + u^3 = 0. \quad (4)$$

*Electronic address: brazhnyi@ciifc.ul.pt

†Electronic address: konotop@ciifc.ul.pt

‡Electronic address: kuzmiak@ure.cas.cz

Let us consider the boundary of the BZ, i.e. $|k| = \pi a_0/L$. As it is known (see e.g. [11]) stationary solitary wave solutions subject to zero boundary conditions $\lim_{|\tilde{x}| \rightarrow \infty} u(\tilde{x}, \tilde{t}) = 0$, exist only if \mathcal{E} belongs to a gap of the spectrum of the underlying linear equation (4). For the sake of definiteness, below we are dealing with the first lowest forbidden gap, which upper and lower edges will be denoted as $\mathcal{E}^{(1)}$ and $\mathcal{E}^{(2)}$, respectively when $\mathcal{E}^{(1)} < \mathcal{E}^{(2)}$ (see an example in Fig. 1d). Thus the frequency of the matter soliton satisfies the condition $\mathcal{E}^{(1)} < \mathcal{E} < \mathcal{E}^{(2)}$. Then a small-amplitude bright matter soliton can be excited in the vicinity of the upper band edge $\mathcal{E}^{(2)}$ [6], with $\mathcal{E}^{(2)} - \mathcal{E} > 0$. For the next consideration it is important to mention that an envelope soliton can also exist if $\mathcal{E} > \mathcal{E}^{(2)}$. In that case however, the soliton is created against a moving carrier wave background (with $|k| < \pi a_0/L$ and $v_2 \neq 0$) and thus it moves in space with the velocity v_2 . In the frame moving with the group velocity of the carrier wave background one can write down the envelope soliton solution of Eq. (1) in a form

$$\psi_s(X, T) = \frac{1}{2} \sqrt{m_2} N \frac{\exp\left(\frac{i}{8} m_2 N^2 T\right)}{\cosh\left[\frac{1}{2} m_2 N (X - v_2 T)\right]} \quad (5)$$

with $\sigma = -1$, $\alpha = 2$, $m_2 > 0$, and $N = \int_{-\infty}^{\infty} |\psi_s|^2 dx$ being the number of particles.

Strictly speaking Eq. (5) is a solution of the unperturbed NLS equation (1) with v_2 and m_2 constants. Since, however, the parameters are changing slowly in space, the simplified picture based on the analytic form (5) appears to be good enough for qualitative understanding various phenomena.

a. Matter wave acceleration. Let us first consider linear modulation of the lattice amplitude (see Fig. 1a)

$$V_\epsilon = (1 - \epsilon^{3/2} \tilde{x}) \cos(2\tilde{x}). \quad (6)$$

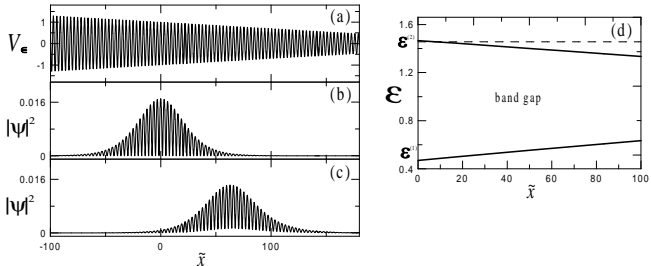


FIG. 1: (a) The inhomogeneous periodic potential V_ϵ and (d) corresponding band structure with $\epsilon = 0.02$. (b) The initial profile of the condensate near the upper bound of the gap for $\mathcal{E} = 1.46$ and $\epsilon = 0$ and (c) profile of the condensate at time $t = 100$ with $\epsilon = 0.02$.

It can be seen from the Figs. 1b,d that in the vicinity of the origin, i.e. near $\tilde{x} = 0$, a bright static gap soliton with $v_2 = 0$ can be created (an example of its shape

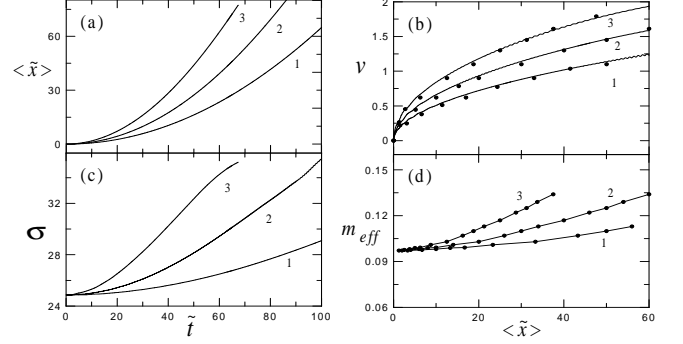


FIG. 2: (a) Dynamics of the coordinate of the soliton center of mass computed as $\langle \tilde{x} \rangle$, where angular brackets stand for the average over the space. (b) Dependences of the carrier wave group velocity v_2 obtained directly from the periodic structure (dots) and velocity of the soliton center of mass obtained from the direct numerical simulations (solid line). (c) Evolution of the dispersion of the soliton. (d) Dependence of the effective mass m_{eff} on the coordinate of the soliton center of mass. Curves 1, 2 and 3 correspond to $\epsilon = 0.02, 0.03$, and 0.04 , respectively.

is shown in Fig. 1b). Due to nonzero extension of the soliton, it partially occupies the space where the soliton energy falls into allowed band – see Fig. 1d – and thus corresponds to running linear waves. This is a reason for a soliton to start to move toward the region with a narrower gap, i.e. in the positive direction. Since it is assumed that in the leading approximation the energy of the soliton is conserved, the group velocity of the background increases and, therefore, soliton velocity grows with the coordinate of the soliton center and gives rise to a soliton acceleration – see Fig. 2b. An example of dynamics of the coordinate of the center of the mass of the condensate $\langle \tilde{x} \rangle$ and its dispersion $\sigma = (\langle \tilde{x}^2 \rangle - \langle \tilde{x} \rangle^2)^{1/2}$ are shown in Fig. 2a,c obtained by numerical integration of Eq. (3) (hereafter angular brackets stand to spatial average). From this figure one can see that soliton indeed undergoes acceleration in such a way that the soliton velocity follows the change of the group velocity of the background. Simultaneously, the dispersion of the soliton increases as it is shown in Fig. 2c. From the first sight this result does not resemble a model given by Eq. (5) because according to this model the soliton width should decrease as the effective mass increases. The explanation of the apparent discrepancy is in the fact that the group velocity of the background is of unity order, while change of the effective mass is rather slow, and thus soliton (5) cannot adjust adiabatically the change of the band structure. Thus effectively, at some point \tilde{x}_1 , the solution still corresponds to some effective mass at earlier stages, say at \tilde{x}_0 , $\tilde{x}_0 < \tilde{x}_1$ and thus is less than the effective mass computed from the band structure, i.e. $m_2(\tilde{x}_1) < m_2(\tilde{x}_0)$. As a result the wave packet after arriving at the point \tilde{x}_1 does not represent a pure solitary wave, and thus in the process of evolution loses some

number of particles. This process continues as soliton moves to the region with small potential depth, as it is observed in Fig. 1c. Alternatively one can explain the discrepancy between the behavior of the soliton width and the effective mass shown in Fig. 2d by taking into account a monotonically increasing group velocity in the range over which the soliton wave packet extends. Then the soliton wave front has larger velocity than the velocity of its tail, which this leads to spreading of the pulse.

b. Oscillation of the matter wave in a lattice subject to parabolic modulation. Let us consider now a soliton dynamics (the initial profile is shown in Fig. 3b) in a lattice modulated by a parabolic function

$$V_\epsilon(\tilde{x}) = [1 + \epsilon^{5/2}(\tilde{x} - \Delta\tilde{x})^2] \cos(2\tilde{x}) \quad (7)$$

which is shown in Fig. 3a. The band gap structure of this potential is depicted in Fig. 3c. Now one observes oscillations of the condensate cloud – see Fig. 4. The accelerating part of this motion (when the soliton is moving toward the center of the parabolic potential) is explained by the previous example. Having passed the central part of the potential the motion is decelerating and at some point the velocity of the center of mass of the cloud becomes zero. This occurs in the vicinity of a point where the energy of the soliton falls into the forbidden gap. Thus one can speak about Bragg reflection of the soliton, from inhomogeneous periodic potential.

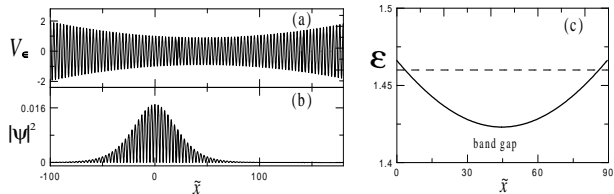


FIG. 3: (a) The inhomogeneous periodic potential V_ϵ and (c) corresponding upper edge of the first band gap for $\epsilon = 0.02$ and $\Delta\tilde{x} = 45$. (b) The initial profile of an envelope soliton (the same as in Fig. 1a).

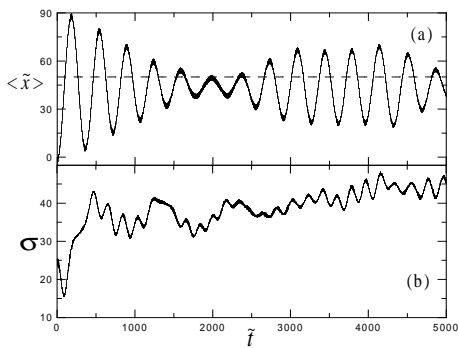


FIG. 4: (a) Dynamics of the center of mass of the BEC and (b) dispersion of the soliton. Parameters the same as in Fig. 3. The dashed line corresponds to $\langle \tilde{x} \rangle = \Delta\tilde{x}$.

There are two features of the soliton dynamics to point out in this case. First, in contrast to the case of the linear modulation, at the initial stages the dispersion decreases – see Fig 4b. This happens due to the fact that due to the large extension of the soliton, the leading part of the wave packet undergoes Bragg reflection and moves in the negative direction while the soliton center still moves in the positive direction, what results in compression of the packet. The second feature demonstrated in Fig. 4a can be identified as beatings of the mean coordinate of the wave packet. In order to explain this effect, we first observe that the higher frequency we designate it ν , obtained numerically is $\nu \approx 0.017$, is the effective linear oscillator frequency associated with the effective parabolic potential, the later being estimated as $2\epsilon^{5/4} \approx 0.014$ (the observed discrepancy is due to the fact that one with a modulated periodic potential, rather than with a real parabolic potential). The envelope soliton is characterized by the internal frequency ω_{int} , which is related to its width ℓ as it satisfies $\omega_{int} = 1/(2m_2\ell^2)$ – see Eq. (5) where $\ell^{-1} = 2/(m_2N)$ and $\omega_{int} = m_2N^2/8$. In the case depicted in Figs. 3, 4, one estimates $\ell \approx 50$ and, taking into account that $m_{eff} \approx 0.1$ – see Fig. 1d one obtains $\omega_{int} \approx 0.002$. That implies $\omega_{int}/\nu \approx 8.6$, which corresponds to 9 fast oscillations per one period of the slow beatings observed in Fig. 4a.

c. Interaction of a soliton with a defect. The phenomenon of the Bragg reflection of a soliton can be also observed in the system where the optical lattice is locally modulated, as it is shown in Figs. 5a and 6a – see also Eqs. (8), (9). In these cases we also start with numerically obtained bright solitons, but adding now some initial velocity v with respect to the stationary background which is introduced in terms of the phase factor $\psi(\tilde{x}, 0)e^{iv\tilde{x}/2}$. We are interested in the scattering process at different initial velocities, which are assumed to be small enough - $v \ll 1$. Hereafter local deformations of the lattice will be referred to as lattice defects.

Let us start with the case of local increase of the lattice depth, the situation modeled by the following potential

$$V_\epsilon(\tilde{x}) = [1 + e^{-\epsilon^{5/2}(\tilde{x} - \Delta\tilde{x})^2}] \cos(2\tilde{x}). \quad (8)$$

In this case the soliton is reflected from the defect. This is the effect of the Bragg reflection which shown in Fig. 5b and is discussed above in more detail. Thus, the defect described by the Eq. (8) can be classified as a repulsive one.

Let us consider now a situation when the depth of the periodic potential is locally decreased (Fig. 6a)

$$V_\epsilon(\tilde{x}) = [1 - e^{-\epsilon^{5/2}(\tilde{x} - \Delta\tilde{x})^2}] \cos(2\tilde{x}), \quad (9)$$

which leads to local narrowing of the forbidden gap. By using arguments based on the bandgap structure one may agree that the modulation described by the Eq. (9) acts as an attractive impurity, and thus some number of atoms should be captured by such a defect, in the case when an

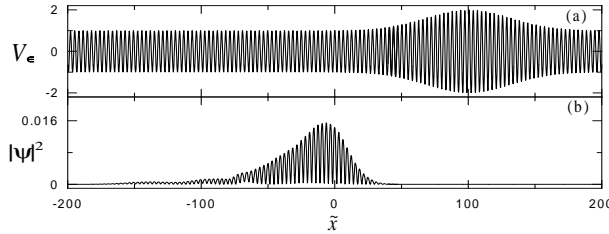


FIG. 5: (a) Periodic potential with defect given by Eq. (8). Parameters of the defect are $\epsilon = 0.05$ and $\Delta\tilde{x} = 100$. (b) Profile of the reflected soliton with the initial velocity $v = 0.1$ at time $t = 150$. The initial soliton profile is the same as in Fig. 1b.

initial kinetic energy of the condensate is small enough. This is exactly what we observe in numerical simulations shown in Fig. 6b. The higher velocity matter waves pass through the defect without substantial changes – see Fig. 6c.

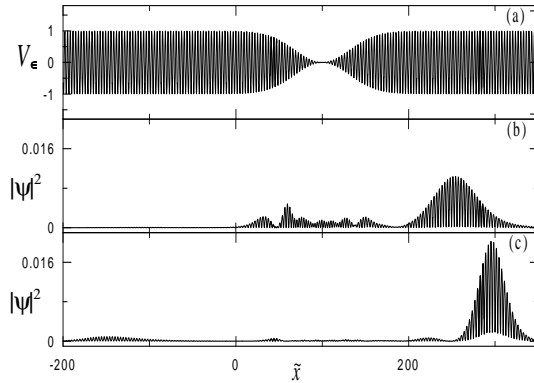


FIG. 6: (a) Periodic potential with the defect given by Eq. (9). Parameters of the defect are $\epsilon = 0.05$ and $\Delta\tilde{x} = 100$. Profiles of the soliton with different initial velocities $v = 0.1$ (b), and $v = 0.3$ (c) after time $t = 300$ and $t = 190$, respectively. The initial soliton profile is the same as in Fig. 1a.

In conclusion, we have shown that in modulated optical lattices that can be created by using quasi-monochromatic laser beams, one can effectively manage matter solitons as they accelerate, decelerate, oscillate or undergo the reflection depending on the type of the modulation introduced. Since the above processes are controlled by the periodic structure, not only dynamical, but also other properties of matter waves such as a chemical potential and an effective mass (and thus a width) can be changed. Although in a particular dynamical process a matter wave can lose its solitonic properties, the effective mass approach provides a qualitative explanation of the main features of the soliton dynamics, if the wave packet possesses a substantially larger extension than the lattice period.

Work of V.A.B. has been supported by the FCT fellowship SFRH/BPD/5632/2001. V.V.K. acknowledges support from the European grant, COSYC n.o. HPRN-CT-2000-00158. Cooperative work was supported by the bilateral agreement GRICES/Czech Academy of Sciences and COST P11 Action.

[1] B. P. Anderson and M. A. Kasevich, *Science* **282**, 1686 (1998).
[2] F.S. Cataliotti, S. Burger, C. Fort, P. Maddaloni, F Minardi, A. Trombettoni, A. Smerzi, M. Inguscio, *Science* **293**, 843 (2001).
[3] M. Greiner, I. Bloch, O. Mandel, T.W. Hänsch, T. Esslinger, *Phys. Rev. Lett.* **87**, 160405 (2002).
[4] M. Greiner, O. Mandel, T. Esslinger, T.W. Hänsch, I. Bloch, *Nature* **415**, 39 (2002).
[5] M. Krämer, L. Pitaevskii, and S. Stringari, *Phys. Rev. Lett.* **88**, 180404 (2002).
[6] see e.g. V. V. Konotop and M. Salerno, *Phys. Rev. A* **65**, 021602(R) (2002) and references therein.
[7] see e.g. M. Cristiani, O. Morsch, J.H. Müller, D.

Ciampini, and E. Arimondo, *Phys. Rev. A* **65**, 063612 (2002), and references therein.
[8] O. Morsch, J.H. Müller, M. Cristiani, D. Ciampini, E. Arimondo, *Phys. Rev. Lett.* **87**, 140402 (2001).
[9] B. Eiermann, P. Treutlein, Th. Anker, M. Albiez, M. Taglieber, K.-P. Marzlin, and M.K. Oberthaler, *Phys. Rev. Lett.* **91**, 060402 (2003).
[10] R.G. Scott, A.M. Martin, T.M. Fromhold, S. Bujkiewicz, F.W. Sheard, and M. Leadbeater, *Phys. Rev. Lett.* **90**, 110404 (2003).
[11] G.L. Alfimov, V.V. Konotop, M. Salerno, *Europhys. Lett.* **58**, 7 (2002).